

# Frequency Reconfigurable Near-Zero Refractive Index Material for Antenna Gain Enhancement Applications

Ren Wang<sup>1</sup>, Tao Tang<sup>2</sup>, Melad M. Olaimat<sup>3</sup>, Yuanzhi Liu<sup>4</sup>

<sup>1</sup>School of Electronic Science and Engineering, University of Electronic Science and Technology of China, Chengdu 611731, P. R. China, [r.wang05@protonmail.com](mailto:r.wang05@protonmail.com)

<sup>2</sup>College of Electronic Engineering, Chengdu University of Information Technology, Chengdu 610025, China, [tangt@cuit.edu.cn](mailto:tangt@cuit.edu.cn)

<sup>3</sup>Department of Renewable Energy, University of AL Albayt, Al-Mafraq, Jordan, [melad.olaimat@aabu.edu.jo](mailto:melad.olaimat@aabu.edu.jo)

<sup>4</sup>The Edward S. Rogers Sr. Department of Electrical and Computer Engineering, University of Toronto, Toronto, ON, M5S 3G4, Canada, [yuanzhi.liu@mail.utoronto.ca](mailto:yuanzhi.liu@mail.utoronto.ca)

**Abstract**— In this paper, a planar near-zero refractive index material (NZRIM) consisting of an outer loop with four symmetrical quarter-rings is proposed. The quarter-rings are connected to the outer loop by two symmetrical microstrip lines on the opposite side. The backside of the substrate has mutually central split microstrip lines. By loading adjustable capacitor between the split in the center of the backside of the substrate, the resonance frequencies of the proposed NZRIM can be controlled and thus the epsilon-near-zero (ENZ) frequency bands change correspondingly. According to the specific frequency bands of its metamaterial characteristics, the proposed NZRIM can be mounted above the surface of different antennas with different operation bands for 5G applications. Results show that the proposed NZRIM can enhance the forward radiation gain of antennas.

**Index Terms**— NZRIM, ENZ, frequency reconfigurable, gain enhancement.

## I. INTRODUCTION

The near-zero refractive index material (NZRIM) refers to a class of materials with a refractive index close to or equal to zero [1]. Because the refractive index can be expressed as  $n = \sqrt{\epsilon_r \mu_r}$ , the NZRIM can be broadly classified into two types: single-zero materials, where only  $\epsilon_r$  or  $\mu_r$  is close to zero, and double-zero materials, where both  $\epsilon_r$  and  $\mu_r$  are close to zero. Single-zero materials can also be subdivided into epsilon-near-zero (ENZ) media and mu-near-zero (MNZ) media. Besides, because the special properties of this kind of material are determined by the structure of its constituent units rather than the materials themselves, modifying the unit configuration can result in a near-zero refractive index.

When an electromagnetic wave propagates with a specific angle from a near zero refractive index material into the air, it is equivalent to being incident from a low refractive index material to a high refractive index material. According to the Snell's law, the electromagnetic wave's angle of refraction will decrease, causing the electromagnetic wave's emission direction in the air to be deflected in the direction normal to the intersection, resulting in the electromagnetic wave's convergence [2].

Due to its superior physical features, the NZRIM has recently emerged as a key development field in metamaterials, and it is widely used in disciplines such as electromagnetic wave control [3]–[5] and

antenna gain enhancement [6], [7]. For example, the zero-index metamaterials (ZIMs) have been used to improve the gain of many types of antennas [8]–[13].

In this work, a planar NZRIM based on ENZ element is designed, which presents epsilon-near-zero (ENZ) characteristic at various frequency bands from 1GHz to 10GHz. The proposed design consists of an outer loop and four symmetrical quarter-rings. The quarter-rings are connected to the outer loop by two symmetrical microstrip lines on either side. On the backside of the substrate, there are split mutually central microstrip lines. The resonance frequency of the proposed NZRIM can be controlled by loading adjustable capacitor between the split in the center of the backside of the substrate, and the ENZ frequency band will change correspondingly. According to the characteristics of near-zero frequency reconfigurable of the material, it can be applied to different antennas with different operation frequency bands to enhance its forward radiation gains.

## II. CONFIGURATION AND RESULTS

The suggested NZRIM structure, as shown in Fig. 1, is printed on the Rogers 5880 substrate with a thickness of 0.25mm and a relative permittivity of 2.2. It consists of a loop, which is located at the outer edge of the design, and four symmetrical quarter-rings separated by two slots. Four vertical and horizontal arms that are connected with the outer loop and the four separated quarter-rings. The other end of the four vertical and horizontal arms are connected in the middle. The dimensions of the design are given in Table I. As Fig. 1 (b) shows that there are split mutually central microstrip lines on the backside of the substrate. Inductors or capacitors can be mounted on the split to change the resonance properties of the device.

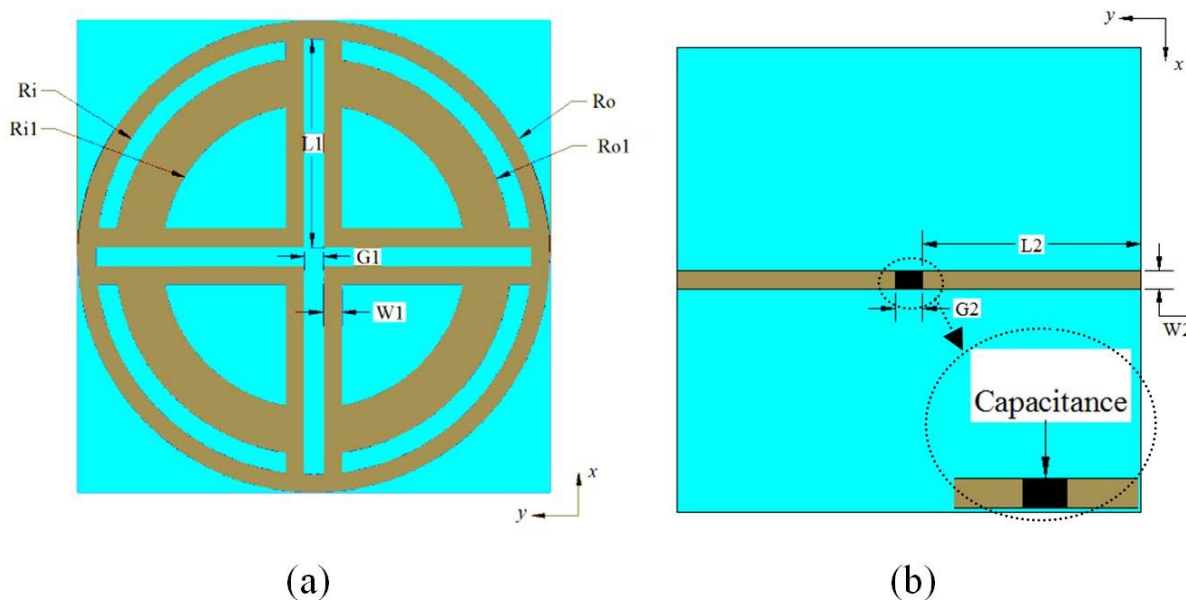


Fig. 1. The configuration of the NZRIM: (a) front view, (b) back view.

The relative permittivity and permeability, as well as the refractive index can be obtained from the S-parameters of the material [14]. Fig. 2 (a) displays the relative permittivity  $\epsilon_r$  and the refractive index  $n$  of the proposed structure. It can be seen that the relative permittivity is close to zero in many frequency bands. For most cases, the relative permeability of the material is equal to 1. According to the relationship between the refractive index and the relative permittivity, it is clear that the refractive

index of the structure should also be close to zero in the corresponding frequency band. Consequently, the proposed structure has the properties of NZRIM.

TABLE I. DETAILED DIMENSIONS OF THE NZRIM (MM)

Parameters	Values	Parameters	Values	Parameters	Values
$R_o$	25	$L_1$	22	$G_1$	2
$R_i$	23	$L_2$	24	$G_2$	2
$R_{o1}$	21	$W_1$	2		
$R_{i1}$	16	$W_2$	2		

As shown in Fig. 2 (b), the loading of capacitors with different capacitance will affect the material features of the design to construct a frequency reconfigurable NZRIM. The frequency ranges with a refractive index around zero can be adjusted accordingly. Unsurprisingly, the frequency reconfigurability of the NZRIM can be simply acquired by altering the loading capacitor. Fig. 3 presents the relative permittivity and permeability of the NZRIM element, which demonstrates that the proposed structure exhibiting ENZ properties in very wide frequency ranges ( i.e., from 2GHz to 10GHz except a few frequency points).

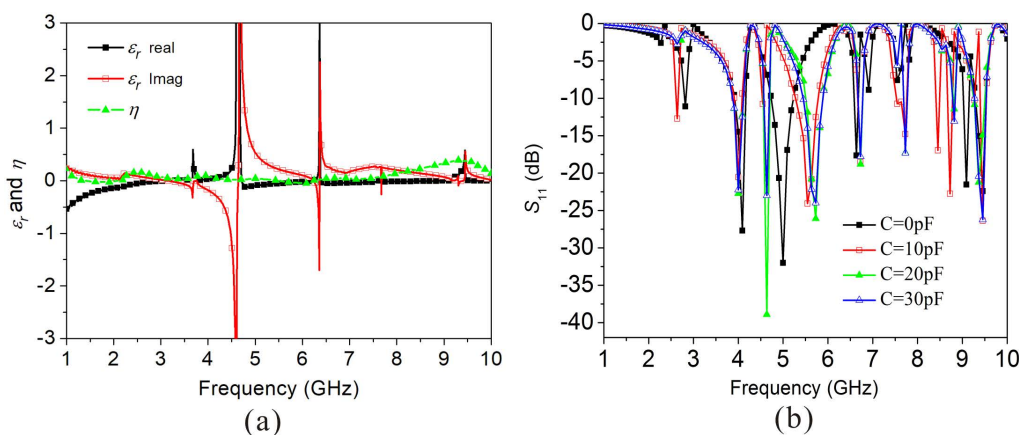


Fig. 2. The relative permittivity and the refractive index as well as the  $S_{11}$  response of the NZRIM with different capacitances: (a) relative permittivity and the refractive index, (b)  $S_{11}$  response.

It should be highlighted that the optimum ENZ material is obtained when the loaded capacitance is 20pF as its permittivity is the most stable and closest to 0 among these cases. Furthermore, loading the capacitance improves the singularity of the relative permeability, but the improvement of magnitude is limited.

As shown in Fig. 1, the front side of the NZRIM is symmetrical, but there is only one microstrip line used on the back side. Therefore, the setup style of the ports will affect the material property of the proposed structure. For instance, in the process of investigation of the permittivity of the structure, if the ports are set as parallel to the back split microstrip line or orthogonal to the back split microstrip line. Fig. 4 shows the permittivity with 20pF load in two different cases, from which we can note that the permittivity of the structure will not near to 0, but less than 0 at many frequencies with two large ridge points when the ports are orthogonal to the split microstrip line.

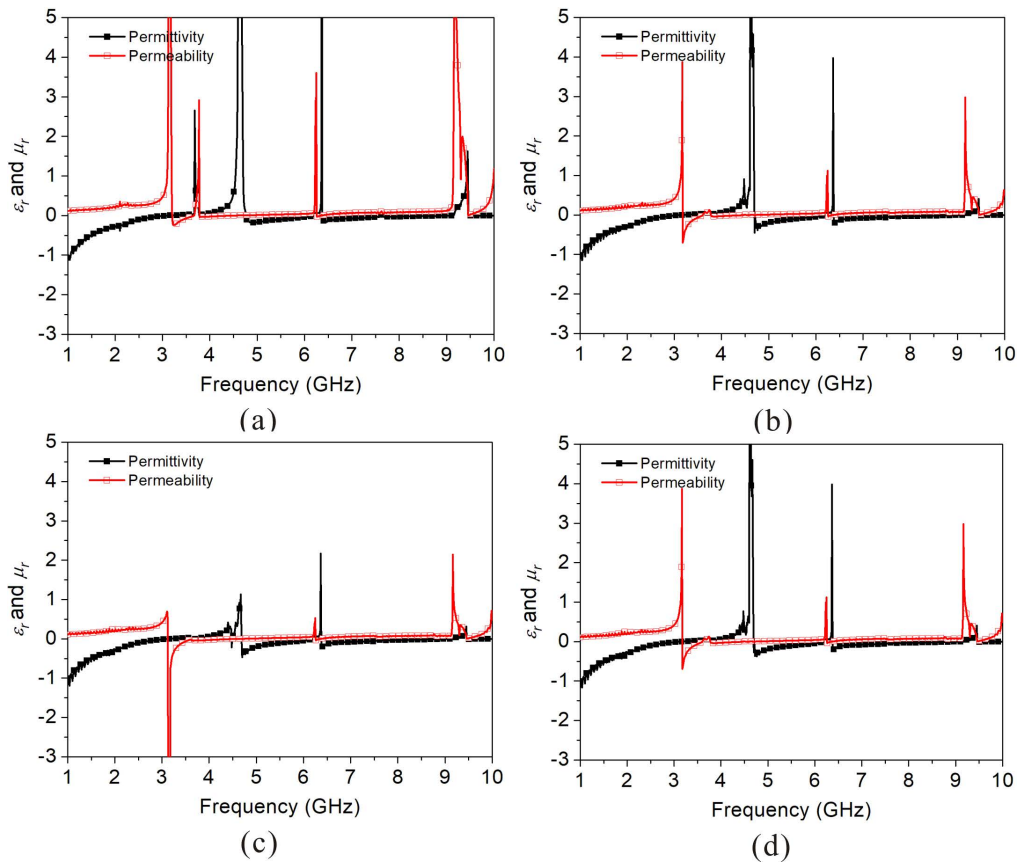


Fig. 3. The relative permittivity and the permeability of the NZRIM with different capacitors: (a)  $C=0\text{pF}$ , (b)  $C=10\text{pF}$ , (c)  $C=20\text{pF}$ , (d)  $C=30\text{pF}$ .

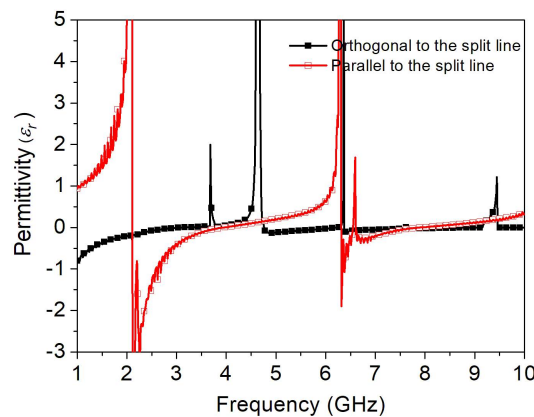


Fig. 4. The permittivity of the NZRIM with different setup of the ports.

### III. GAIN ENHANCEMENT

From the boundary conditions, the normal component of the electric displacement vector on the surface of the ideal medium satisfies the continuous condition. Then, the electric field intensity at the interface between air and the NZRIM should satisfy  $\epsilon_0 E_{n0} = \epsilon_r E_{nr}$ , where  $\epsilon_0$  is the permittivity of the air,  $E_{n0}$  is the normal component of the electric field in the air,  $\epsilon_r$  is the relative permittivity of the NZRIM, and  $E_{nr}$  is the normal component of the electric field in the NZRIM. Since the proposed NZRIM exhibits ENZ characteristics in frequency bands of interest and  $\epsilon_r \approx 0$ , then there should be  $E_{nr} \gg E_{n0}$ . Furthermore, according to the Snell's law:  $n_i \sin(\theta_i) = n_0 \sin(\theta_0)$ , when the electric field is

emitted from the NZRIM into the air, i.e.,  $n_i \approx 0$  and  $n_0 = 1$ , for any incident angle  $\theta_i$ , there is  $\theta_0 \approx 0$ . This means that a source placed in a NZRIM will radiate electromagnetic waves perpendicular to the surface of the NZRIM and maintain good directivity. This phenomenon known as the highly directional radiation effect of the NZRIM [15]. The enhancement of antenna gain by NZRIM can be explained both by the boundary conditions and the Snell's law together. The field radiated by the antenna will be amplified by the NZRIM, and then radiated out again after passing through the NZRIM, due to the high directivity of the NZRIM, the forward gain of the antenna will be enhanced.

To evaluate the gain enhancement due to the proposed NZRIM, two patch antennas that work in the sub-6GHz 5G bands are utilized. The first patch antenna resonates at 3.5GHz and the second one resonates at 4.9GHz. The substrates are employed for the two patch antennas are the same with the used for the NZRIM. Both antennas are feed by 50ohm matched microstrip line. The size of the radiation patch is  $27 \times 35\text{mm}^2$  and  $19.3 \times 25\text{mm}^2$  respectively. Fig. 5 illustrates the setup of the suggested NZRIM and the patch antenna. The NZRIM is placed at  $h=21.4\text{mm}$  and  $h=17\text{mm}$  (about  $\lambda/4$  for 3.5GHz and 4.9GHz respectively) from the first and the second patch antenna's front face respectively.

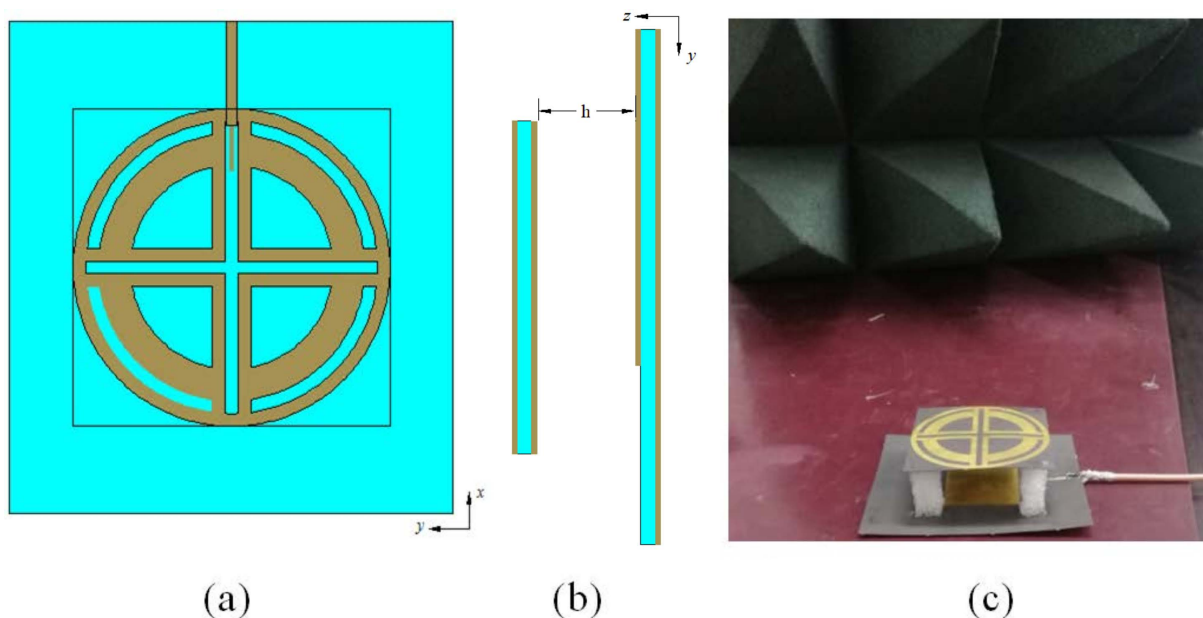


Fig. 5. The setup of the NZRIM with antenna and the prototype:(a) front view, (b) side view, (c) prototype.

Figures 6 and Fig. 7 show the  $S_{11}$ , radiation patterns, and forward gain of the antennas with and without the NZRIM. As can be seen from the Fig. 6 (a) and (b), the resonant frequency point of the first patch antenna will increase when loaded with this NZRIM. The resonant point of the antenna increases from 3.48GHz to 3.52GHz and the -10dB bandwidth of the antenna also increases. While the resonant frequency point of the second patch antenna keeps unchanged when loaded with this NZRIM. However, the bandwidth of the antenna increases significantly.

In addition, the forward gains of both antennas are enhanced and the radiation directivity of both antennas is significantly improved after loading the NZRIM, as shown in Fig. 7. For instance, the first antenna in the band ranges from 3.05GHz to 3.80GHz and the second antenna in the band ranges from 4.51GHz to 5.62GHz are improved after loading the NZRIM. The first antenna's maximum forward gain has been improved from 7.81dBi to 8.38dBi at 3.5GHz and the half-power beamwidth (HPBW) is reduced nearly by 24% from 71.3 degrees to 54.2 degrees, which means that the radiation directionality

of the antenna is significantly improved. While the second antenna's maximum forward gain has been improved from 7.65dBi to 8.51dBi at 4.9GHz corresponding to the HPBW is reduced more than 34% from 78.2 degrees to 51.3 degrees.

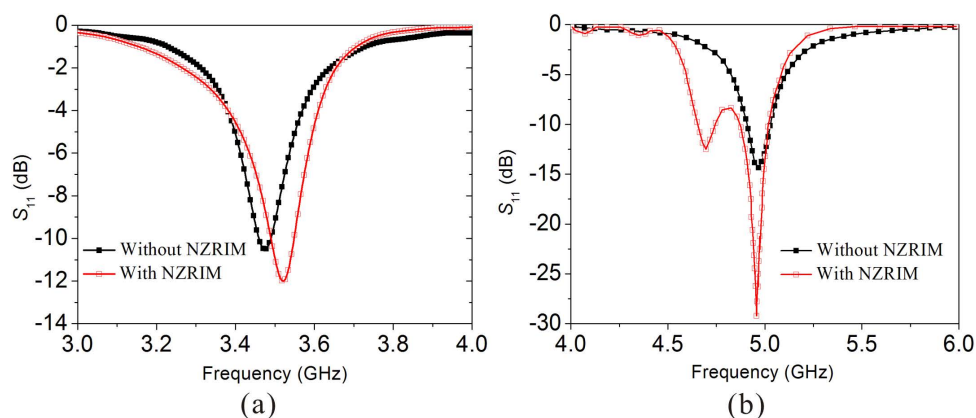


Fig. 6. The  $S_{11}$  of the patch antenna with and without the NZRIM: (a) first antenna, (b) second antenna.

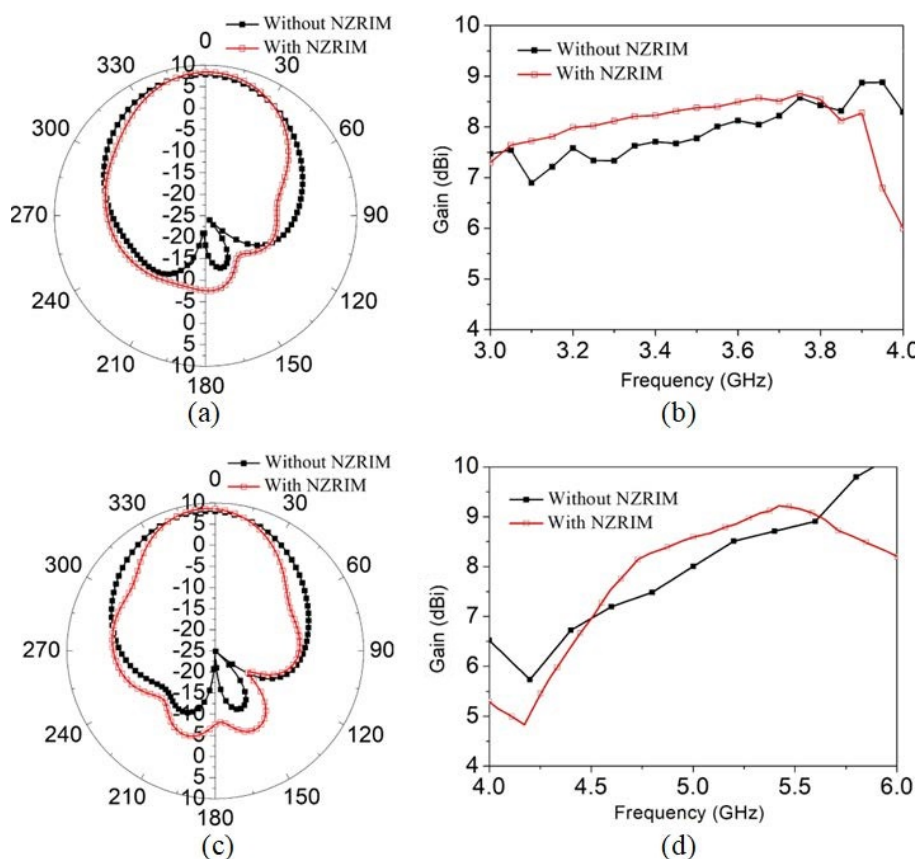


Fig. 7. The radiation patterns and forward gains of the patch antenna with and without the NZRIM: (a) radiation pattern of the first antenna, (b) gains VS frequency of the first antenna, (c) radiation pattern of the second antenna, (d) gains VS frequency of the second antenna.

The proposed NZRIM element can be used to construct an NZRIM array to be applied to improve the gain of an antenna array as well. For example, for a  $2 \times 2$  antenna array consisted of the first patch antenna, the NZRIM element proposed in this work is placed directly above each antenna in the same way as in Fig. 5. At a distance of 21.4mm, the maximum forward gain of the array antenna has been



increased from 13.2dBi to 14.8dBi at 3.5GHz, while the HPBW has been decreased from 15.8 degrees to 15.1 degrees.

#### IV. DISCUSSIONS AND MEASUREMENTS

The proposed structure given in Fig. 1 can be approximated as the equivalent circuit shown in Fig. 8. The equivalent circuit can be divided into three parts: First, the surface metal structure can be equated to four inductors and capacitors in parallel cells, with one capacitor connected in series between the cells. Second, the back side microstrip line can be equated to a capacitor and inductor in parallel and then in series with a capacitor. Third, the metal parts of the surface and back can be equated to a capacitor in parallel with the above circuit. Finally, the additional external capacitor in the middle split of the back side is also connected in parallel with the above circuit.

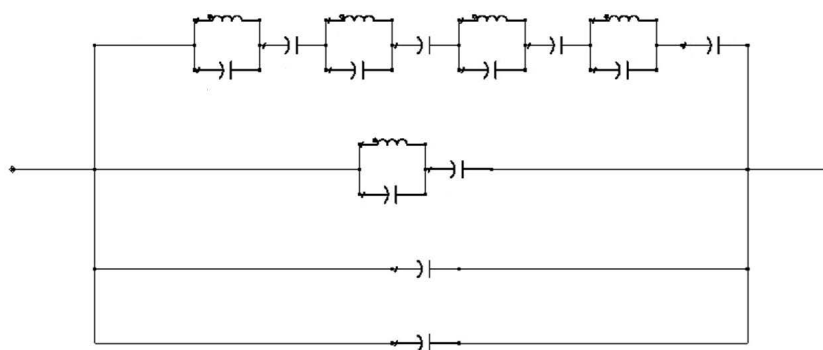


Fig. 8. Equivalent circuit of the proposed structure with loading capacitor.

The  $S_{11}$  of the first three parts of the equivalent circuit of the proposed structure is shown in Fig. 9 (a), and the  $S_{11}$  response of the whole equivalent circuit when loaded with different additional external capacitors in the middle split of the back side is shown in Fig. 9 (b). From Fig. 9 (b), we can note that the resonant properties can be controlled by changing the value of the additional capacitors of the back side.

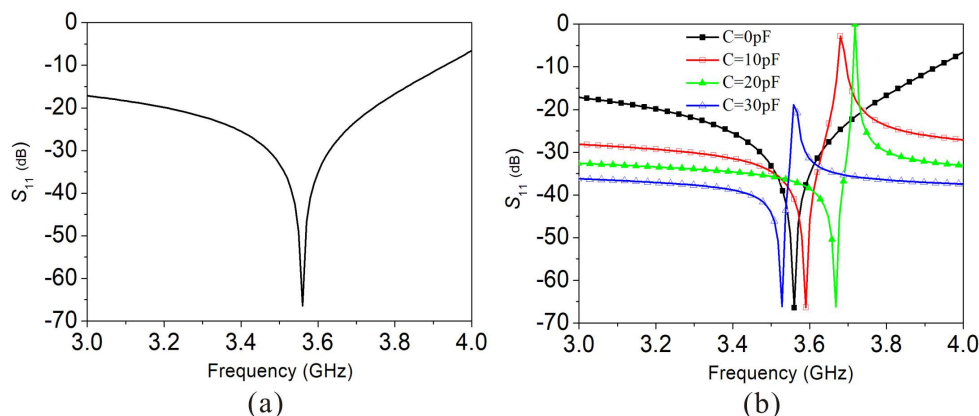


Fig. 9. The response of the  $S_{11}$  of the equivalent circuit: (a)  $S_{11}$  of the equivalent circuit, (b)  $S_{11}$  with different capacitors.

Figure 10 presents the E-fields in the substrate for loading different additional capacitors, while the electric field distribution in the substrate can reflect the variation of the capacitance of the equivalent circuit of the structure. From Fig. 10, it can be seen that the electric field intensity increases and then decreases with the increase of the loaded capacitance, and then increases again. When the value of the



loading capacitor is 20pF, the electric field intensity in the substrate is the smallest, indicating that the equivalent capacitance of the structure at this condition is the smallest.

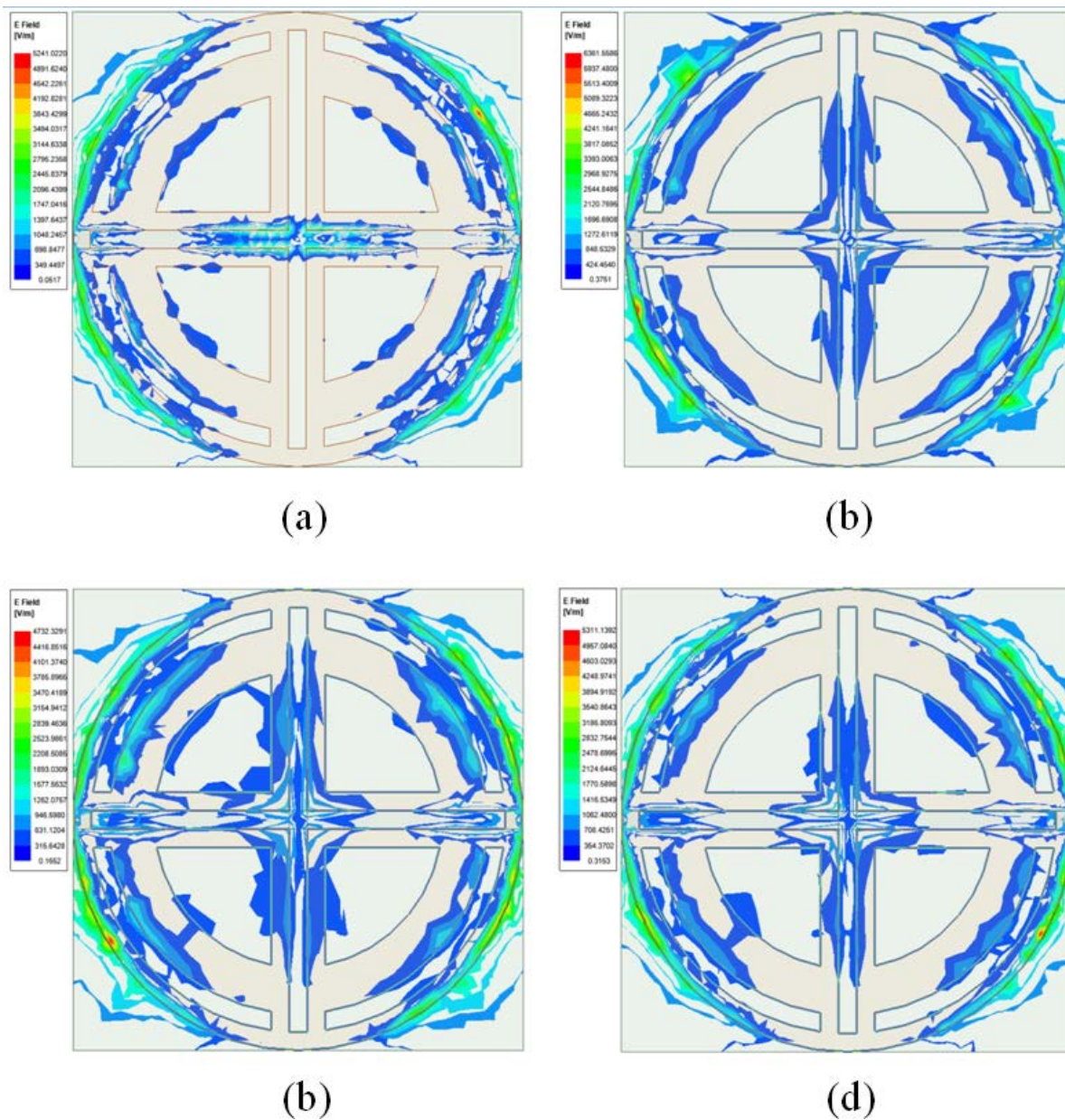


Fig. 10. E-field distribution in the substrate with different capacitors: (a)  $C=0\text{pF}$ , (b)  $C=10\text{pF}$ , (c)  $C=20\text{pF}$ , (d)  $C=30\text{pF}$ .

The placement of the NZRIM also affects the gain of the antenna. As discussed before, since the structure of the front side of this NZRIM is symmetrical, it is mainly the placement direction of the microstrip lines with the split on the backside that affects the antenna gain. As can be seen from the Fig. 11, the gain is enhanced when the microstrip line on the back of the NZRIM is parallel to the antenna feed line.

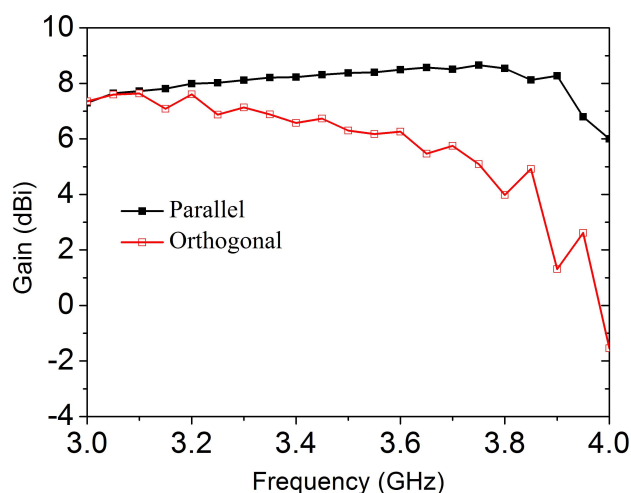


Fig. 11. Gains with different placement of the NZRIM.

As depicted in Fig. 12 (a), when this NZRIM is replaced with an air substrate, the structure also exhibits ENZ characteristics in many frequency bands. After the medium is changed to air, the structure is also placed 21.4mm in front of the first antenna. The effect on the forward gain of the antenna is shown in Fig. 12 (b). As can be got from the Fig. 12, when the substrate is changed to air, the relative permittivity of the structure is closer to zero in the higher frequency band, and also there is no singularity in the band of interest. Furthermore, the antenna gain enhancement in the higher frequency range is superior to the substrate-based structure.

The distance between the NZRIM and the front side of the antenna has an impact on the antenna performances. Taking the first antenna as an example, the distance between the NZRIM and the antenna front side is set to be  $\lambda/8$ ,  $\lambda/4$ ,  $\lambda/2$  and  $\lambda$  for 3.5GHz, namely about 10.7mm, 21.4mm, 42.8mm and 85.7mm, the detail responses of the antenna are given in Table II.

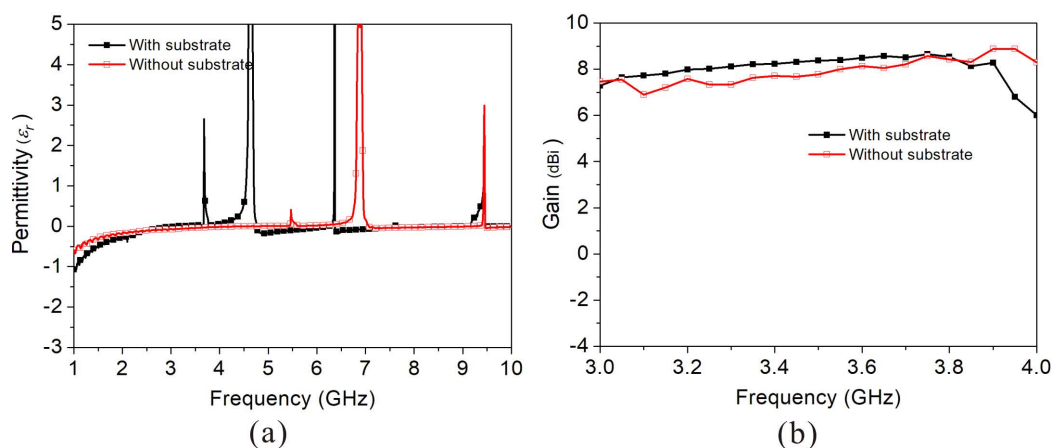


Fig. 12. The material characters and the gains of the patch antenna with the NZRIM with or without substrate: (a) material characters, (b) gains.

As illustrated in Fig. 5, the proposed NZRIM and patch antenna were fabricated to evaluate the gain enhancement capability of the NZRIM. The NZRIM was loaded with plastic screws at 21.4mm and 17mm high from the first and the second antenna front side. As displayed in Table III, the measured resonant frequencies of the two antennas are 3.58GHz and 4.95GHz, respectively, and the gains at 3.5GHz of the two antennas are 7.32dBi and 7.64dBi, respectively.

TABLE II. ANTENNA PERFORMANCES WITH THE NZRIM WITH DIFFERENT DISTANCES

Distance (mm)	Resonate frequency (GHz)	Gain at 3.5GHz (dBi)	3dB beam width (degree)
10.7	3.31	8.85	59.5
21.4	3.52	8.46	56.7
42.8	3.46	9.21	58.9
85.7	3.46	8.41	53.5

TABLE III. MEASURED RESULTS

	First antenna		Second antenna	
	With the NZRIM	Without the NZRIM	With the NZRIM	Without the NZRIM
Resonate frequency (GHz)	3.58	3.53	4.95	4.91
Gain (dBi)	7.32	6.65	7.64	6.47

## V. CONCLUSIONS

An NZRIM element is proposed in this paper to provide near zero relative permittivity in wide frequency bands. Studies show that by loading different capacitors between the split on the back microstrip line of the NZRIM, the frequency response of the NZRIM can be adjusted, the frequency bands with the near-zero refractive index change correspondingly. This characteristic is also demonstrated by the equivalent circuit model. Simulation results show that the relative permittivity of the structure stays close to zero in most frequency bands from 1 to 10GHz when the loaded capacitance is 20pF. Two antennas working at 5G bands are employed to validate its gain enhancement function. Results show that the proposed NZRIM can improve the antenna maximum gain in the band ranging from 3.05GHz to 3.80GHz, and in the band ranging from 4.51GHz to 5.62GHz. The proposed structure can also apply for an antenna array to improve its radiation performances. Since the structure can keep the relative permittivity close to zero in many frequency bands and its material characters can adjust by loading different capacitor, the structure can be used in many frequency bands to improve the radiation gain of the antenna element and antenna array.

## ACKNOWLEDGMENTS

This work was supported in part by the Key Research and Development Project of Guangdong Province (No. 2020B0101080001), and in part by the Key Laboratory of Antenna and Microwave Technology.

## REFERENCES

- [1] S. S. Islam, M. R. I. Faruque, and M. T. Islam, "A near zero refractive index metamaterial for electromagnetic invisibility cloaking operation," *Materials*, vol. 8, no. 8, pp. 4790–4804, 2015.
- [2] Z. Haider, M. U. Khan, and H. M. Cheema, "A dualband zeroindex metamaterial superstrate for concurrent antenna gain enhancement at 2.4 and 3.5 ghz," *IETE Journal of Research*, pp. 1–11, 2020.
- [3] K. Sreejith and V. Mathew, "Optical properties of planar and annular ternary superconducting photonic crystals in near-zero-permittivity operation range," *Journal of Superconductivity and Novel Magnetism*, vol. 32, no. 8, pp. 2397–2407, 2019.
- [4] T. Suzuki, T. Sato, M. Sekiya, and J. C. Young, "Epsilon-near-zero three-dimensional metamaterial for manipulation of terahertz beams," *Applied optics*, vol. 58, no. 11, pp. 3029–3035, 2019.
- [5] P. Dawar and M. A. Abdalla, "Near-zero-refractive-index metasurface antenna with bandwidth, directivity and front-to-back radiation ratio enhancement," *Journal of Electromagnetic Waves and Applications*, pp. 1–19, 2021.

- [6] S. S. Efazat, R. Basiri, and S. Jam, "Optimization based design of a wideband near zero refractive index metasurface for gain improvement of planar antennas in the terahertz band," *Optical and Quantum Electronics*, vol. 52, no. 12, pp. 1–16, 2020.
- [7] Y. Ma, P. Wang, X. Chen, and C. Ong, "Near-field plane-wave-like beam emitting antenna fabricated by anisotropic metamaterial," *Applied Physics Letters*, vol. 94, no. 4, p. 044107, 2009.
- [8] J. P. Turpin, Q. Wu, D. H. Werner, B. Martin, M. Bray, and E. Lier, "Low cost and broadband dual-polarization metamaterial lens for directivity enhancement," *IEEE Transactions on Antennas and Propagation*, vol. 60, no. 12, pp. 5717–5726, 2012.
- [9] A. Bakhtiari, "Investigation of enhanced gain miniaturized patch antenna using near zero index metamaterial structure characteristics," *IETE Journal of Research*, pp. 1–8, 2019.
- [10] Y. Liu, X. Guo, S. Gu, and X. Zhao, "Zero index metamaterial for designing high-gain patch antenna," *International Journal of Antennas and Propagation*, vol. 2013, 2013.
- [11] M. Sun, Z. N. Chen, and X. Qing, "Gain enhancement of 60-ghz antipodal tapered slot antenna using zero-index metamaterial," *IEEE Transactions on Antennas and Propagation*, vol. 61, no. 4, pp. 1741–1746, 2012.
- [12] D. Li, Z. Szabó, X. Qing, E.-P. Li, and Z. N. Chen, "A high gain antenna with an optimized metamaterial inspired superstrate," *IEEE transactions on antennas and propagation*, vol. 60, no. 12, pp. 6018–6023, 2012.
- [13] Z. H. Jiang, Q. Wu, D. E. Brocker, P. E. Sieber, and D. H. Werner, "A low-profile high-gain substrate-integrated waveguide slot antenna enabled by an ultrathin anisotropic zero-index metamaterial coating," *IEEE Transactions on Antennas and Propagation*, vol. 62, no. 3, pp. 1173–1184, 2013.
- [14] D. R. Smith, D. C. Vier, T. Koschny, and C. M. Soukoulis, "Electromagnetic parameter retrieval from inhomogeneous metamaterials," *Phys. Rev. E*, vol. 71, p. 036617, 2005.
- [15] J. Luo and Y. Lai, "Epsilon-near-zero or mu-near-zero materials composed of dielectric photonic crystals," *Science China Information Sciences*, vol. 56, pp. 1–10, 12 2013.